BIOPHYSICAL ACTIVE CONTOURS FOR CELL TRACKING I: TENSION AND BENDING

Jacques Pecreaux[1*], *Christophe Zimmer*[2], *Jean-Christophe Olivo-Marin*[2]

1. Max Planck Institute of Molecular Cell Biology and Genetics,
PfotenhauerStr. 108, 01307 Dresden, Germany
2. Quantitative Image Analysis Group,
Institut Pasteur, 25 rue du Docteur Roux, 75015 Paris, France

ABSTRACT

Automatic segmentation and tracking of biological objects from dynamic microscopy data is of great interest for quantitative biology. A successful framework for this task are active contours, curves that iteratively minimize a cost function, which contains both data-attachment terms and regularization constraints reflecting prior knowledge on the contour geometry. However the choice of these latter terms and of their weights is largely arbitrary, thus requiring time-consuming empirical parameter tuning and leading to sub-optimal results. Here, we report on a first attempt to use regularization terms based on known biophysical properties of cellular membranes. The present study is restricted to 2D images and cells with a simple cytoskeletal cortex underlying the membrane. We describe our new active contour model and its implementation, and show a first application to real biological images. The obtained segmentation is slightly better than standard active contours, however the main advantage lies in the self-consistent and automated determination of the weights of regularization terms. This encouraging result will lead us to extend the approach to 3D and more complex cells.

Index Terms— Biophysics, Image segmentation, Biomedical image processing

1. INTRODUCTION

Current biological research increasingly relies on quantitative studies of large data sets, an important part of which are in the form of images obtained with various modern microscopy techniques. Dedicated image processing methods able to extract and characterize biological objects are of great interest to ensure a level of speed and reproducibility beyond the reach of a purely human analysis.

The present work is motivated by the goal to track and outline moving cells from videomicroscopy image sequences. For this purpose, we and others have adopted the framework of active contours and deformable models (see [1] for a review). Active contours [2] are curves that evolve in the image domain to iteratively minimize a suitably defined cost function, or energy. The equilibrium state of the contour provides a segmentation of the object, and tracking is achieved by repeating the process on consecutive frames of an image sequence. The energy to be minimized contains image-dependent terms designed to be minimal when the curve follows the object boundaries, and image-independent terms that act as regularizers in ill posed problems and are needed to reduce the effect of image noise on the computed segmentation.

These image-independent terms represent a priori information on the contour in the form of a penalty on specific characteristics of the curve, such as its smoothness, length, area or similarity to a reference shape. For example, the widely used regularization energy of [2] is the integral of the squared first and second derivatives of the curve position with respect to the curve parameter. These two terms can be interpreted as tension and rigidity energies, respectively. However, no physical justification has been given for using these terms. The model [2] is thus applied to a variety of images without considering the physical properties of the objects to be extracted. This is an important limitation of most active contour approaches. Indeed, one must expect sub-optimal segmentations for most images, since the image-independent energy will always favour the same shapes (e.g. a curve vanishing to a point in the model of [2]) irrespective of the objects of interest. Furthermore, individual terms in the regularization energy are weighted by arbitrary coefficients (hyperparameters), which in practice must be fine-tuned by the users, often in a laborious trial and error process.

To overcome these limitations, it seems natural to seek energies based on known physical properties of the objects to be extracted. One can thus expect to develop active contours with fewer arbitrary parameters and improved performances on specific classes of objects and images, perhaps at the price of loosing some applicative generality.

Although there have been efforts to introduce physical properties in deformable models for medical imaging applications, no comparable work has been done for biological imaging. Here, focusing on cell imaging, we report our first attempt to develop a new active contour model with regularization energies based on biophysical properties of cell membranes. Section 2 briefly recalls the classical active contour model of [2], and describes our new active contour model with biophysical energy. Section 3 gives details of our implementation. Section 4 provides experimental results and discussion, and section 5 the conclusion.

2. A BIOPHYSICAL ACTIVE CONTOUR MODEL

2.1. Representation of the contour

In this first attempt, and for simplicity, we have chosen to work on 2D images. The contour will be represented by a curve $\mathbf{C}$ with coordinates $(x(p,\tau,t), y(p,\tau,t))$, where $p \in [0,1]$ is a space parametrisation, τ is a virtual time and t is the physical time corresponding to the frame number in a temporal image sequence. The physical time is needed here, in contrast to almost all active contour methods, to account for "memory" effects (see below). Independent variables will now be implicit when obvious.

The level set technique [3, 4], (in which curves are represented implicitly as the zero level set of a scalar function defined on the image) is a popular alternative to the parametric representation. However, only purely geometric characteristics of the curves can be ex-

*We thank Vincent Galy for the images used in this paper. JP acknowledges funding from Human Frontiers Sciences Program Organisation.

pressed in this representation. Although this is generally considered an advantage because it makes curve evolution independent of change in parametrization, it is not adapted here, because we will need to express a tension/stretching energy, which depends on the changes in distance between material points (see below). Approximation of that term in order to obtain a non parametrization-dependant term will be investigated in further work to use the level-sets formalism.

2.2. Standard active contour energy

As a basis for comparisons, we consider active contours minimizing the following cost function (energy), previously introduced in [5]:

$$E = E_I + E_R^S \quad (1)$$

$$E_I = \lambda_O \iint_{\text{outside}(\mathbf{C})} (I - c_2)^2 \, dx\, dy + \lambda_I \iint_{\text{inside}(\mathbf{C})} (I - c_1)^2 \, dx\, dy \quad (2)$$

$$E_R^S = \frac{1}{2} \int_0^1 \left[\alpha \left(\frac{\partial \mathbf{C}}{\partial p} \right)^2 + \beta \left(\frac{\partial^2 \mathbf{C}}{\partial p^2} \right)^2 \right] dp \quad (3)$$

Here $I = I(x, y)$ is the intensity of the image at the point (x, y), c_I and c_O are the average intensity respectively inside and outside the contour, λ_I, λ_O, α and β are the hyperparameters. This model combines the data attachment term from [6] and the standard regularization terms of [2], and is well suited to segmenting deformable fluorescent cells [5].

We stress again, however, that the regularization energy E_R^S is not based on the physical properties of the cell membranes.

2.3. Biophysically motivated active contour energy

We now propose to replace the regularization energy E_R^S with the following energy:

$$E_R^P = \int_0^1 \left[\sigma \left| \frac{dl}{dp} - \left(\frac{dl}{dp} \right)_0 \right| + \kappa c^2 \frac{dl}{dp} \right] dp \quad (4)$$

In the following, we will define the notations and give physical justifications for this energy and for ranges of values of the associated parameters, and provide explicit expressions allowing us to compute contour evolution.

2.3.1. Tension energy

The first term in (4) is the tension energy due to stretching of the cell membrane. The tension term was first proposed in soft matter thermodynamics to account for the energy due to the interface. More precisely, one unit of surface of interface has an energetical cost σ. In the case of a cell membrane, the tension is due to the bilayer of lipids, which are amphilic molecules [7, 8]. The tension value σ is estimated to be in the range of $10^{-7} - 10^{-4}$ J/m^2 under non extreme conditions [9].

Another contribution to the tension energy comes from the cytoskeleton, a network of actin and tubulin polymers and intermediate filaments that exerts mechanical forces within the cell. Here, we will only consider the cortex of actin underlying the membrane; other cytoskeletal components are usually embedded deeply inside the cell [10] and thus negligible for relatively small cell deformations. The energetic cost of stretching the actin cortex can however also be ignored, because elongation in one direction is almost exactly compensated by contraction in the perpendicular direction (Poisson ratio in 2D for an actin layer is very close to $\nu_{2D} \simeq 1$ since $\nu_{3D} \simeq 0.5$ from 3D measurements [11, 12]. Experiments [9, 13] support also this result.

We note that the main contribution of the cytoskeleton to the energy is associated with the shear stress [14], estimated for red blood cells at $\mu \simeq 1.5 \times 10^{-2}$ J.m^{-2} [11], however we cannot include it since we are only considering the cell contour in 2D.

For a 3D membrane S, the tension energy (due to the strech-ing of the membrane) is $\iint_S \sigma \, |dS - dS_0|$, where dS is the current surface element and dS_0 the corresponding surface element in the reference shape S_0. Since dS and dS_0 must refer to the very same piece of surface material, they contain the same Lagrangian points. The reference shape S_0 is defined as the zero stress shape [7, 8]. In the 2D setting of this work, we simply express the tension energy as $\oint_{\mathbf{C}} \sigma \, |dl - dl_0| = \int_0^1 \left| \frac{dl}{dp} - \left(\frac{dl}{dp} \right)_0 \right| dp$ with $dl = \left(\frac{dl}{dp} \right) dp = \left| \frac{\partial \mathbf{C}}{\partial p} \right| dp$ the contour length element and dl_0 the elementary length at the same material point in the reference shape.

The reference shape introduces a memory effect in the model, that is not present in standard active contours [2, 3, 6]. This reference shape is not fixed, but dominated by the more recent configurations, as the cytoskeleton progressively reorganizes to relax stresses [10]. Here, we make the simple assumption that the shape memory decays exponentially with time:

$$\left(\frac{dl}{dp} \right)_0 (t) = \int_{-\infty}^{t} \frac{1}{T} \frac{dl}{dp}(t_1) \exp \frac{t_1 - t}{T} \, dt_1 \quad (5)$$

where T is a characteristic time scale on the order of minutes [10].

2.3.2. Bending energy

The bending term in (4) is due to the curvature c of the membrane. In lipid bilayers, the shape of individual lipids combined with the lipidic composition of each leaflet result in a preferred, so called spontaneous curvature c_0 [7, 8]. However, c_0 has typical values of only $c_o \sim 10$ m^{-1} [15], which is negligible compared to typical membrane curvatures $c \simeq 10^5 m^{-1}$ for cells with typical sizes of $\sim 10 \mu m$.

The weight κ in (4) is the bending modulus. Typical values are $\kappa \simeq 2 \times 10^{-19}$ J for red blood cells (with a cytoskeleton of spectrin) [16], and $2 \times 10^{-20} - 3 \times 10^{-19}$ J for lipids [9].

Classically, in the Area Difference Elasticity (ADE) model [17, 18], three contributions are identified for the curvature energy: the energy due to the mean curvature, the gaussian curvature and the global curvature. We will only keep the former energy, since the integrals over the closed 2D contour $\mathbf{C}$ of the gaussian curvature and the global curvature are both constants according to the Gauss-Bonnet and the "turning tangent" theorems, respectively [19].

Thus the curvature energy of interest here reduces to:

$$\oint_{\mathbf{C}} \kappa c^2 \, dl = \int_0^1 \kappa c^2 \left| \frac{d\mathbf{C}}{dp} \right| dp$$

where the curvature is given by $c = \left(\frac{\partial^2 y}{\partial p^2} \frac{\partial x}{\partial p} - \frac{\partial^2 x}{\partial p^2} \frac{\partial y}{\partial p} \right) / \left| \frac{\partial \mathbf{C}}{\partial p} \right|^3$.

3. IMPLEMENTATION OF CONTOUR EVOLUTION

We now wish to compute the evolution of $\mathbf{C}$ that minimizes the new energy $E = E_I + E_R^P$ from (2) and (4).

3.1. Modification of tension term

The tension term in (4) contains a modulus that has no derivative when $\frac{dl}{dp} = \left(\frac{dl}{dp} \right)_0$. To remedy this, we replace the tension term by

the following expression:

$$\frac{1}{2}\sigma\left(\Delta l\,\mathrm{erf}\left(\frac{\Delta l}{\xi}\right)+\frac{\xi}{\sqrt{\pi}}e^{-\frac{\Delta l^2}{\xi^2}}\right)\quad\text{with}\quad\Delta l=\frac{dl}{dp}-\left(\frac{dl}{dp}\right)_0$$

With $\xi = 0.5$, we have a quadratic behaviour around $\frac{dl}{dp} = \left(\frac{dl}{dp}\right)_0$ and far from this point a linear behaviour as desired.

3.2. Reference shape initialization

The initial reference shape of a cell needed to compute (5) and (4) is not known at the onset of an image sequence. However, because of the finite memory time T (see section 2.3.1), a reference shape can be built from the first $M = T * fps$ frames of the series of images, where fps is the frame rate. In order to do this, we progressively increase the tension energy by replacing σ in (4) by an effective tension $\sigma_e = \frac{j}{M}\sigma$ for each frame j ($j \leq M$).

3.3. Evolution equation

We follow the standard gradient descent approach [2, 3, 6], to minimize the energy $E_I + E_R$ by letting the contour evolve until convergence according to:

$$\frac{\partial \mathbf{C}}{\partial \tau} = -\frac{\delta\left(E_I + \lambda E_R\right)}{\delta \mathbf{C}} \tag{6}$$

The explicit evolution equations for $E_R = E_R^S$ were given in [5]. For $E_R = E_R^P$, unfortunately, the explicit form of (6) is too complex to be shown here[1]. We automatically generated it from (2) and (4) using the symbolic calculator Mathematica (Wolfram Research). This expression was then discretized and introduced in an iterative numerical scheme written in Matlab (The Mathworks).

4. EXPERIMENTAL RESULTS

4.1. Procedure

We now report a first test of our approach on a time series of real biological cell images shown in Fig. 1. This series shows a one cell embryo of the nematod *Caenorhabditis elegans* observed with fluorescence microscopy [2]. We wish to compare our biophysically motivated active contour model defined by (4), (2) and (6) to the more standard non physical active contour model [5] defined by (3), (2) and (6).

4.1.1. Segmentation quality criterion

In order to quantify the quality of segmentations obtained with standard active contours and the present model, we use a manually drawn curve $\mathbf{C}_0$ around the cell of Fig. 1 as a ground truth. We then define a measure of segmentation error $\mathcal{Q}$ as the integral of the distance of each contour point $\mathbf{C}(p)$ to the ground truth curve $\mathbf{C}_0$. The lower $\mathcal{Q}$, the better the segmentation. $\mathcal{Q}$ is always non-negative and $\mathcal{Q} = 0$ indicates a perfect segmentation. For each segmentation $\mathbf{C}$, $\mathcal{Q}$ is computed numerically using an interpolation scheme.

[1]Here, λ is a constant coefficient needed to convert physical quantities into non-dimensional quantities: $\lambda = 9.2 \times 10^{10}$ for the biophysical active contours and $\lambda = 1$ for the standard active contours

[2]We used β-tubulin protein labelled with Green Fluorescent Protein

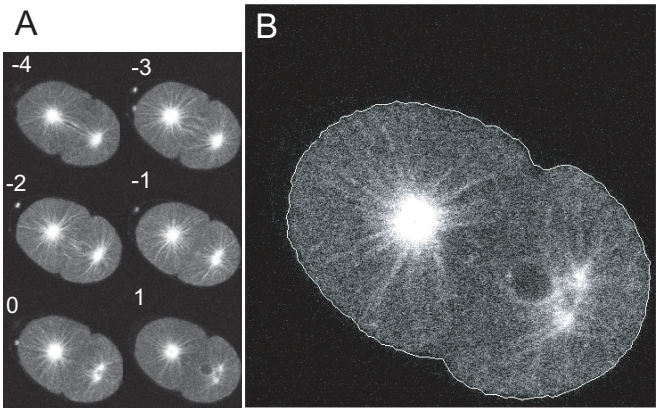

Fig. 1. Segmentation of a fluorescent *C. elegans* cell by the proposed method. A. the sequence of 6 frames used for the initialization of shape memory and segmentation. B. Segmentation of frame # 1.

4.1.2. Processing the image series

Although the segmentations will be evaluated only on frame #1, the biophysical active contours were run sequentially on frames # -4 through # 1. This is necessary to initialize the shape memory (see section 3.2 above). For computation of the reference shape by (5), we use an estimated memory time based on known cell division time of $T = 150$s. The standard active contours, which contain no memory term, were run only on frame # 1.

4.1.3. Screening for the best parameters

A meaningful comparison of the two active contour models requires setting the hyperparameters to adequate non-arbitrary values. For this purpose, we vary the hyperparameters logarithmically over wide ranges of values and choose the set of parameters that minimizes the error $\mathcal{Q}$.

Since this work is concerned with the regularization energy and not primarily with the data attachment terms (which are identical in both models), we can set $\lambda_O = \lambda_I = 1.4$ in all experiments and only vary the regularization hyperparameters. For the standard model, the ranges of the hyperparameters tested are as follows: $\alpha = 4\times10^{-4}$ to 10^2 and $\beta = 6.4\times10^{-5}$ to 10. This range of parameters spans 6-7 orders of magnitudes around values providing empirically reasonable segmentations.

For the biophysical active contours, the range of tested hyperparameters are $\kappa = 2 \times 10^{-22} - 2 \times 10^{-13}$ J and $\sigma = 5 \times 10^{-10} - 5 \times 10^{-1}$ J.m^{-2}. Note that both ranges cover 9 orders of magnitude, whereas the physically predicted values for κ and σ span only about 2 and 3 orders of magnitude, respectively (see sections 2.3.1 and 2.3.2). Therefore, an important test of the validity of our approach is to determine if hyperparameters that achieve good segmentations are also inside the physically realistic range.

4.2. Results

4.2.1. Segmentation quality

Fig. 1 shows the segmentation obtained by our biophysical active contours with the empirically obtained best set of parameters (see section 4.1.3). The obtained error $\mathcal{Q}$ was 5 % smaller than for the best segmentation obtained with the standard active contours. This improvement may seem marginal, but note that $\mathcal{Q}$ is only a global

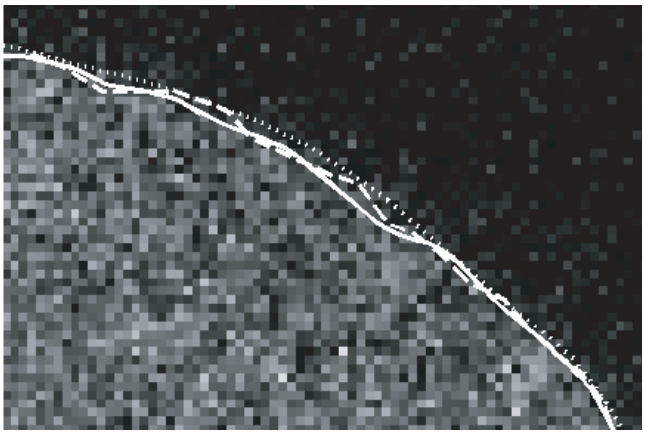

Fig. 2. Detail of Fig. 1 segmented by the biophysical active contours (solid curve). For comparison, see the result of segmentation by standard active contours [5] (dotted curve) and the manual ground-truth segmentation (dashed curve).

measure averaged over the entire cell shape. Fig. 2 shows that our algorithm performs notably better than standard active contours in detecting small structures of the cell membrane shape. This result suggests that curvature and tension are more suited as regularization energies for cell image segmentation than first and second derivatives [2, 5]. This is not surprising since the new regularization energies introduced here are the very same energies that control the shape of the real membrane.

4.2.2. Hyperparameter prediction

A second, perhaps more important result pertains to the hyperparameters achieving the best segmentations. With our model, we obtain an optimal parameter ratio $\frac{\sigma}{\kappa} = 2.5 \times 10^{12}$ m^{-2}. This number falls nicely within the range $3 \times 10^{11} - 5 \times 10^{15}$ m^{-2} predicted by physics (see sections 2.3.1 and 2.3.2), although, as mentioned above, this range is much smaller than the range of tested parameters. This is an encouraging confirmation that biophysical considerations are successful at predicting ranges of hyperparameters that contain the optimal values for cell image segmentations.

5. CONCLUSION

We have presented a new regularization energy for active contours based on biophysical knowledge of cell membrane properties. We showed on a real image that this model can give slightly better segmentations than active contours with standard regularization terms. However the main advantage of the presented method is its ability to predict (or significantly narrow down) the range of hyperparameters for the regularization terms. This considerably reduces the need for time-consuming empirical tuning of the hyperparameters.

This is the first step in our effort to integrate biophysical knowledge in cell segmentation algorithms by active contours and the reported results are encouraging. We plan to pursue this approach in two main directions : (i) extend the model to the more realistic 3D case, and (ii) take into account other important cell features such as pseudopods, filopods and adhesive focal points. Among other possible extensions are the handling of topological changes and the modeling of image formation to also predict the hyperparameters of the data attachment energy.

6. REFERENCES

[1] C. Zimmer, B. Zhang, A. Dufour, A. Thébaud, S. Berlemont, V. Meas-Yedid, and J-C. Olivo-Marin, "On the Digital Trail of Mobile Cells," *IEEE Signal Proc. Mag.*, vol. 23, no. 5, pp. 54–62, 2006.

[2] M. Kass, A. Witkin, and D. Terzopoulos, "Snakes: Active contour models," *Int. J. Comput. Vis.*, pp. 312–331, 1988.

[3] N. Paragios and R. Deriche, "Geodesic active contours and level sets for detection and tracking of moving object," *IEEE Trans. Pattern Anal. Machine Intell.*, vol. 22, no. 3, pp. 266–280, 2000.

[4] S. Osher and R. Fedkiw, *Level sets methods and dynamic implicit surfaces*, vol. 153 of *Applied mathematical sciences*, Springer-Verlag, New York, 2003.

[5] C. Zimmer and J-C. Olivo-Marin, "Coupled Parametric Active Contours," *IEEE Trans. Pattern Anal. Machine Intell.*, vol. 27, no. 11, pp. 1838–1842, 2005.

[6] T.F. Chan and L.A. Vese, "Active Contours Without Edges," *IEEE Trans. Image Proc.*, vol. 10, no. 2, pp. 266–277, 2001.

[7] P. B. Canham, "The minimum energy of bending as a possible explanation of the biconcave shape of human red blood cell," *Journal of Theoretical Biology*, vol. 26, pp. 61–81, 1970.

[8] W. Helfrich, "Elastic properties of lipid bilayers : theory and possible experiments," *Zeitschrift Naturforschung Teil C*, vol. 28, pp. 693–703, 1973.

[9] W. Rawicz, K. C. Olbrich, T. McIntosh, D. Needham, and E. Evans, "Effect of chain length and unsaturation on elasticity of lipid bilayers," *Biophys. J.*, vol. 79, pp. 328–339, 2000.

[10] B. Alberts, D. Bray, J. Lewis, M. Raff, K. Roberts, and J. Watson, *Molecular biology of the cell*, Garland Publishing Inc., New York, second edition, 1989.

[11] D. H. Boal, *Mechanics of the cell*, Press syndicate of the University of Cambridge, Cambridge, 2002.

[12] J. Howard, *Mechanics of motor proteins and the cytoskeleton*, Sinauer Associates, Sunderland, MA, USA, 2001.

[13] E. Evans, V. Heinrich, F. Ludwig, and W. Rawicz, "Dynamic tension spectroscopy and stength of biomembranes," *Biophys J*, vol. 85, pp. 2342–2350, 2003.

[14] R. Mukhopadhyay, H. W. G. Lim, and M. Wortis, "Echinocyte shapes: bending, stretching, and shear determine spicule shape and spacing," *Biophys J*, vol. 82, no. 4, pp. 1756–72, 2002.

[15] H.-G. Dobereiner, O. Selchow, and R. Lipowsky, "Spontaneaous curvature of fluid vesicles induced by trans-bilayer sugar asymmetry," *Europ. Biophys. J.*, vol. 28, pp. 174, 1999.

[16] S. Svetina, D. Kuzman, R.E. Waugh, P. Ziherl, and B. Zeks, "The cooperative role of membrane skeleton and bilayer in the mechanical behaviour of red blood cells," *Bioelectrochemistry*, vol. 62, no. 2, pp. 107–113, 2004.

[17] H.-G. Döbereiner, E. Evans, M. Kraus, U. Seifert, and M. Wortis, "Mapping vesicle shapes into the phase diagram: A comparison of experiment and theory," *Physical Review E*, vol. 55, pp. 4458–4474, 1997.

[18] U. Seifert, "Configurations of fluid membranes and vesicles," *Advances in Physics*, vol. 46, no. 1, pp. 13–137, 1997.

[19] M. P. Do Carmo, *Differential Geometry of Curves and Surfaces*, Prentice-Hall, 1976.